COMMUNICATION

A hepatocyte-targeting near-infrared ratiometric fluorescent probe for monitoring peroxynitrite during drug-induced hepatotoxicity and its remediation†

Wen-Li Jiang,[a] Yongfei Li,[ab] Wen-Xin Wang,[a] Yi-Ting Zhao,[a] Junjie Fei[a] and Chun-Yan Li [ID] *[a]

A novel hepatocyte-targeting near-infrared fluorescent probe named Gal-NIR is developed. Gal-NIR shows ratiometric response to ONOO⁻ with high sensitivity and selectivity. Moreover, the probe can accurately target the hepatocyte, and thus is used for assessing drug-induced hepatotoxicity and its remediation by using hepatoprotective medicines in living cells and mice.

The liver is an important metabolic organ, which is involved in deoxygenation, storage of liver sugar and synthesis of secreted protein. Moreover, the liver is the major site to convert drugs to various metabolites, and thus is susceptible to drug damage.[1] Drug-induced liver injury (DILI) is the most common concern of acute liver failure, accounting for a substantial portion of acute hepatitis.[2] Due to its unpredictability and acute response, DILI is considered a serious problem related to public health.[3] Peroxynitrite (ONOO⁻), as one of the reactive oxygen species (ROS), is generated from a diffusion-controlled reaction of nitric oxide (NO) and the superoxide radical anion ($O_2^{\bullet-}$).[4] In the liver, ONOO⁻ is the result of drug metabolite-induced mitochondrial toxicity and has long been regarded as a superior biomarker for the prediction and measurement of DILI.[5] Thus, it is crucial to develop accurate analytical methods for the detection of ONOO⁻ in the liver to evaluate DILI and its remediation.

In recent years, small-molecule fluorescent probes have attracted a great deal of attention owing to their intrinsic advantages such as high sensitivity, easy modulation and high spatial resolution imaging in biological samples.[6] To date, a number of fluorescent probes have been developed to detect ONOO⁻.[7] Despite intensive efforts, three main problems still

remain. First, some elegant ONOO⁻ probes can locate in the mitochondria or lysosomes,[7a–c] while a hepatocyte-targeting probe is rare. This is not beneficial for specific detection of analytes in the liver. Second, most of the probes for ONOO⁻ show short excitation and emission wavelength, which is fraught with interference caused by autofluorescence and restricts their applications *in vivo*.[7d,e] Third, only a few ratiometric probes are developed for detecting ONOO⁻ in order to avoid the effect caused by a variety of factors such as instrumental efficiency, temperature and probe concentration.[7f,g] Unfortunately, ratiometric probes suffer from a small emission shift (less than 100 nm) and thus show a small ratio change. Therefore, it is very challenging to construct an ideal hepatocyte-targeting probe with long wavelength and a large emission shift.

It is reported that the asialoglycoprotein receptor (ASGPR) is overexpressed on the surface of mammalian hepatocytes and allows galactose to enter the cells *via* a specific receptor-mediated endocytosis.[8] Very recently, a number of hepatocyte-specific fluorescent probes with galactose have been developed for messenger molecules.[9] For example, Zhu *et al.* developed a hepatoma-selective fluorescent probe based on naphthalimide for HClO in living cells.[9a] Tian *et al.* described a galactosyl azidonaphthalimide probe for selective fluorogenic imaging of hepatocellular H_2S.[9b] Zhang *et al.* reported a hepatocyte-targeting fluorescent sensor based on galactosyl rhodamine for detecting NO in cells and zebrafish.[9c] Although Zhu *et al.* constructed a galactose-appended hepatoma-specific fluorescent probe Gal-NHP for detecting endogenous ONOO⁻ in live HepG2 cells, Gal-NHP with a short emission wavelength (555 nm) is not suitable for imaging *in vivo*.[9d] As far as we know, the hepatocyte-targeting near-infrared (NIR) probe for tracing ONOO⁻ has not been reported yet.

Herein, a hepatocyte-targeting NIR ratiometric fluorescent probe (Gal-NIR) for ONOO⁻ was designed and synthesized by grafting a galactose moiety onto a coumarin-benzopyrylium-based fluorophore (Fig. 1). Owing to the extended π-conjugation, Gal-NIR displays NIR emission. Upon the addition of ONOO⁻, the probe is oxidized and cleaved to acquire coumarin 343, which has a small π-conjugation system and thus emits green fluorescence. Thus, a ratiometric

[a] *Key Laboratory for Green Organic Synthesis and Application of Hunan Province, Key Laboratory of Environmentally Friendly Chemistry and Applications of Ministry of Education, College of Chemistry, Xiangtan University, Xiangtan, 411105, P. R. China. E-mail: lichunyan79@sina.com*

[b] *College of Chemical Engineering, Xiangtan University, Xiangtan, 411105, P. R. China*

† Electronic supplementary information (ESI) available: Experimental section, synthesis of probes, additional spectral data, response mechanism and supplemental biological assay. See DOI: 10.1039/c9cc07017f

Fig. 1 Design of Probe Gal-NIR to ONOO⁻.

Fig. 2 (a) Absorption spectra of Gal-NIR (5 μM) in the absence (1) and presence (2) of ONOO⁻ (15 μM). Inset: The corresponding color image. (b) Fluorescence spectra of Gal-NIR (5 μM) upon adding various amounts of ONOO⁻ (0, 0.5, 1.0, 2.0, 3.0, 5.0, 7.0, 10.0, 13.0, and 15.0 μM) in PBS buffer solution (pH 7.4). λ_{ex} = 440 nm. Inset: Corresponding fluorescence image under 365 nm ultraviolet radiation. (c) The fluorescence intensity ratio (F_{500}/F_{720}) versus ONOO⁻ concentration. (d) The fluorescence intensity ratio to ONOO⁻ (15 μM) and other various analytes (150 μM). 1: blank, 2: ClO⁻, 3: H_2O_2, 4: ROO•, 5: O_2^-, 6: ·OH, 7: NO, 8: NO_2^-, 9: NO_3^-, 10: H_2S, 11: SO_3^{2-}, 12: HSO_3^-, 13: Cys, 14: Hcy, 15: GSH, and 16: ONOO⁻.

fluorescence response to ONOO⁻ can be obtained with a large emission shift (220 nm). This makes the probe show high sensitivity and selectivity. Moreover, Gal-NIR is applied for ratiometric monitoring of the upregulation of ONOO⁻ during DILI in living HepG2 cells. Furthermore, owing to the probe's NIR emission, Gal-NIR is utilized for imaging the ONOO⁻ level during drug-induced hepatotoxicity and its remediation *in vivo*.

Gal-NIR was synthesized following the synthetic route displayed in Scheme S1 (ESI†). The detailed synthetic steps and characterization are given in the ESI† (Fig. S1–S6). With the probe in hand, the absorption spectra of Gal-NIR in the absence and presence of ONOO⁻ were tested in PBS buffer solution. As shown in Fig. 2a, Gal-NIR itself exhibits a strong absorbance at around 650 nm. After the addition of ONOO⁻, the absorption spectra demonstrate a sharp decrease at 650 nm and an obvious increase at 440 nm. Such an obvious blue shift of 210 nm in the absorption spectra leads to a color change from blue to yellow (inset of Fig. 2a), which enables Gal-NIR to be used for ONOO⁻ detection by the naked eye.

Then, the fluorescence spectra of probe Gal-NIR with varied concentrations of ONOO⁻ were investigated and the results are shown in Fig. 2b. Gal-NIR itself displays fluorescence emission with the peak at 720 nm. With the increase of the ONOO⁻ concentration, the emission at 720 nm decreases and the emission at 500 nm increases gradually under excitation at 440 nm. A large emission shift (220 nm) indicates that the two emissions are well separated and the fluorescence changes from black to green (inset of Fig. 2b). When 15 μM ONOO⁻ is added, the fluorescence intensity ratio (F_{500}/F_{720}) shows 72-fold enhancement. Meanwhile, upon excitation at 650 nm, the fluorescence intensity at 720 nm decreases with the amount of ONOO⁻ (Fig. S7, ESI†). In addition, the probe exhibits an excellent linear relationship with ONOO⁻ concentrations ranging from 0.5 to 15 μM (Fig. 2c), and the detection limit is 0.17 μM (3σ/slope). All these results strongly indicate that Gal-NIR can serve as a highly sensitive probe for ratiometric detection of ONOO⁻.
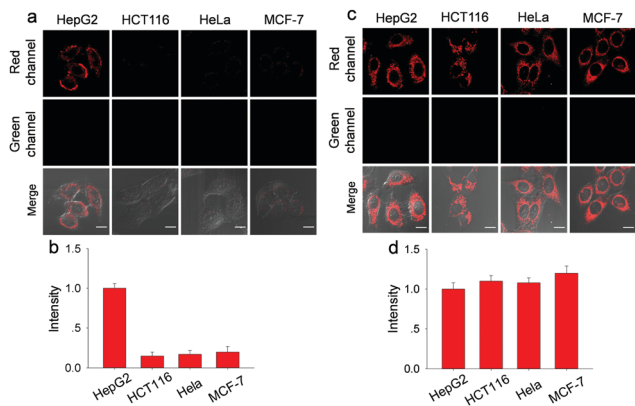
Furthermore, the selectivity of Gal-NIR toward ONOO⁻ was studied by using a series of analytes including reactive oxygen species, reactive nitrogen species, reactive sulfur species and biothiols (Fig. 2d and Fig. S8, ESI†). Only ONOO⁻ (15 μM) causes a large change in the fluorescent intensity ratio (F_{500}/F_{720}). while other analytes display a very small or almost no change even at a higher concentration (150 μM). These results clearly indicate that the probe has excellent selectivity for ONOO⁻, which makes it suitable for detecting ONOO⁻ in a complicated biological environment. In addition, the effect of pH, reaction time and photo-stability were investigated (Fig. S9–S11, ESI†). And a possible response mechanism of Gal-NIR to ONOO⁻ was proposed and proved by the absorption spectra, fluorescence spectra, HPLC and mass spectra (Fig. S12–S15, ESI†).

Before fluorescence imaging, the cytotoxicity of Gal-NIR and Gal-NIR with ONOO⁻ was evaluated in HepG2 cells by conventional MTT assay (Fig. S16, ESI†). A high cell viability (above 90%) is observed after the cells are respectively treated with various concentrations of Gal-NIR (0–30.0 μM) and ONOO⁻ (0–20.0 μM), demonstrating low cytotoxicity of Gal-NIR and Gal-NIR with ONOO⁻. The hepatocyte-specific ability of Gal-NIR was evaluated by respectively incubating human hepatoma cells (HepG2), human colon cancer (HCT116), human cervix cancer (HeLa) and human breast cancer cells (MCF-7) (Fig. 3a and b). Although all the cells are stained by Gal-NIR for 30 min, a strong red fluorescence signal is only found in HepG2 cells, while no obvious fluorescence signal change is seen in the other kinds of cells. This may be because the asialoglycoprotein receptor (ASGPR) is primarily expressed on the membrane of hepatocytes (e.g. HepG2 cells) and can specifically recognize the galactose group in Gal-NIR. In comparison, probe NIR without the galactose group was respectively incubated in these different kinds of cells (Fig. 3c and d). Confocal fluorescence imaging shows that probe NIR could enter the cells and exhibit red fluorescence regardless of the cell types. The above results indicate that Gal-NIR containing the galactose group has excellent hepatocyte-targeting ability.

Fig. 3 Fluorescence imaging of different cells (HepG2, HCT116, HeLa and MCF-7 cells). (a) The cells were treated with Gal-NIR (5 μM) for 30 min. (b) Relative fluorescence intensity of the red channel in a and the fluorescence intensity in HepG2 cells is defined as 1.0. (c) The cells were treated with NIR (5 μM) for 30 min. (d) Relative fluorescence intensity of the red channel in c and the fluorescence intensity in HepG2 cells is defined as 1.0. Scale bar: 10 μm. Red channel: λ_{ex} = 635 nm and λ_{em} = 650−750 nm; green channel: λ_{ex} = 488 nm and λ_{em} = 500−550 nm.

Next, the probe was used for detecting exogenous and endogenous ONOO⁻ in HepG2 Cells (Fig. S17, ESI†).

With wonderful hepatocyte-targeting and cell-imaging ability, Gal-NIR was used to explore drug-induced liver injury (DILI) in HepG2 cells (Fig. 4). It is well-known that acetaminophen (APAP) is a household medication for treating pain and fever.[10] Excessive APAP in the liver can induce hepatotoxicity through the overproduction of ONOO⁻.[11] After the treatment of APAP with increasing concentrations, the fluorescence intensity in the red channel diminishes and the fluorescence intensity in the green channel enhances (Fig. S20, ESI†). When APAP reaches 500 μM, there is a 5.4-fold increase of the fluorescence intensity ratio (F_{green}/F_{red}) compared with the control. The results reveal that intracellular ONOO⁻ is upregulated under the administration of APAP and Gal-NIR is able to detect the change of ONOO⁻ in DILI. Moreover, so many hepatoprotective medicines have been developed for drug-induced hepatotoxicity, such as
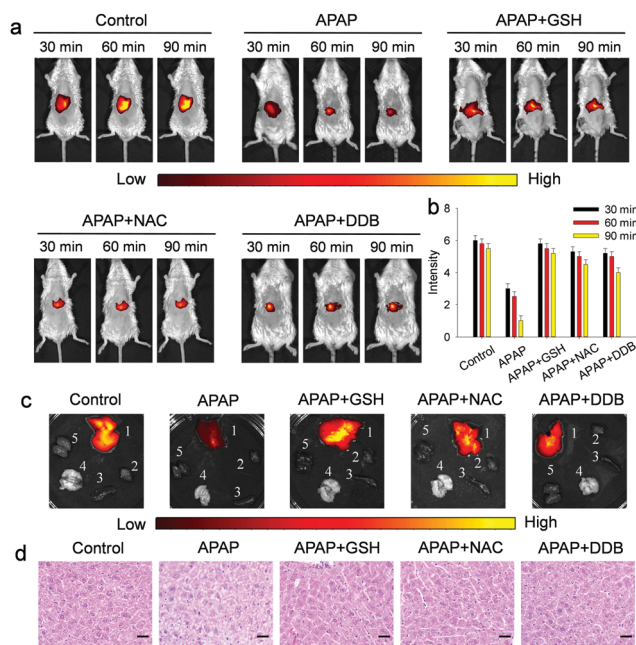
glutathione (GSH), *N*-acetylcysteine (NAC) and biphenyldicarboxylate (DDB).[12] Upon the addition of GSH, NAC or DDB, the fluorescence intensity ratio (F_{green}/F_{red}) decreases. By comparing the changes in the fluorescence signal ratio induced by GSH, NAC, or DDB, GSH may be superior to NAC and DDB as an antidote to APAP toxicity. This may be because GSH can remediate cell injury by the depletion of ONOO⁻ levels. All in all, these imaging experiments illuminate that Gal-NIR can effectively evaluate the remediation effect of medicines for DILI.

On the basis of the probe's NIR optical properties and the desirable results of imaging ONOO⁻ in hepatocytes, Gal-NIR was further utilized to monitor ONOO⁻ *in vivo*. BALB/c mice were used in these experiments and fluorescence imaging was studied only in the red channel. As shown in Fig. S21a (ESI†), the mice injected with Gal-NIR produce fluorescence in the liver, while the mice given injection of NIR display fluorescence in the liver and other parts. After this the mice were sacrificed and the main organs were obtained (Fig. S21b and c, ESI†). For Gal-NIR, the fluorescence is found only in the liver. For NIR, the fluorescence is observed in some other organs such as the kidney and lungs besides the liver. All the results show that the hepatocyte-targeting group is able to guide Gal-NIR to locate in the liver of mice.

Furthermore, the suitability of the probe for assessing drug-induced hepatotoxicity (DILI) and its remediation was examined (Fig. 5). As displayed in Fig. 5a and b, the mice injected

Fig. 4 Fluorescence imaging of APAP-induced hepatotoxicity in HepG2 cells. (a) The cells were treated with Gal-NIR (5 μM) for 30 min. (b) The cells were pretreated with APAP (500 μM) for 12 h and then incubated with Gal-NIR (5 μM) for 30 min. (c−e) The cells were co-incubated with (c) GSH (400 μM), (d) NAC (400 μM) or (e) DDB (400 μM) for 1 h, and then treated with APAP (500 μM) for 12 h, followed by treatment with Gal-NIR (5 μM) for 30 min. (f) Fluorescence intensity ratio (F_{green}/F_{red}) is obtained from image (a−e) and the ratio of image a is defined as 1.0. Scale bar: 10 μm. Red channel: λ_{ex} = 635 nm, λ_{em} = 650−750 nm; green channel: λ_{ex} = 488 nm, λ_{em} = 500−550 nm.

Fig. 5 Fluorescence imaging of APAP-induced hepatotoxicity *in vivo*. (a) Fluorescence imaging of BALB/c mice of control, APAP (500 mg kg⁻¹) alone, APAP (500 mg kg⁻¹) with GSH (400 mg kg⁻¹), NAC (400 mg kg⁻¹), DDB (400 mg kg⁻¹), followed by Gal-NIR (100 μL, 200 μM). Mice imaging was operated only in the red channel: λ_{ex} = 640 nm; λ_{em} = 680−780 nm. (b) Relative fluorescence intensity in a and the lowest fluorescence intensity is defined as 1.0. (c) Fluorescence imaging in the main organs of mice. 1: liver, 2: heart, 3: spleen, 4: lungs, 5: kindey. (d) H&E staining of liver tissues from the above mice. Scale bar: 50 μm.

with APAP show a significant decrease of fluorescence with time, suggesting that Gal-NIR is capable of monitoring $ONOO^-$ in mice with APAP-induced liver injury. And, three hepatoprotective medicines (GSH, NAC and DDB) were injected after APAP-induced hepatotoxicity, and the obvious recovery of fluorescence in the liver is observed. The results prove that the three medicines could offset $ONOO^-$ produced by DILI. Subsequently, the mice were sacrificed and the main organs were recovered (Fig. 5c). The fluorescence imaging clearly indicates that the selective localization of Gal-NIR is in the liver over other organs including the heart, spleen, lungs and kidney. In addition, histological analysis of liver tissues was performed by hematoxylin and eosin (H&E) staining (Fig. 5d). Just like the change in fluorescence, the liver tissues of mice treated with hepatoprotective medicines are closer to the normal state, while the vacuolization of the cells is observed from the injured liver tissues of the APAP-injected mice. All the above experiments confirm that Gal-NIR could not only be hepatocyte-specific, but also be a useful indicator to monitor the biological processes of APAP-induced hepatotoxicity and its remediation by using the three kinds of hepatoprotective medicines *in vivo*.

In conclusion, we have reported a hepatocyte-targeting NIR fluorescent probe (Gal-NIR) for ratiometric detection of $ONOO^-$. The probe is prepared by linking a galactose moiety on a coumarin-benzopyrylium-based fluorophore. Moreover, Gal-NIR shows a large emission shift (220 nm), which is beneficial for enhancing the signal-to-background ratio. Furthermore, the probe exhibits high sensitivity for $ONOO^-$ with a 72-fold increasing ratio and excellent selectivity for $ONOO^-$ over various potential biological analytes. In addition, Gal-NIR can specifically target the hepatocyte, and thus is used for assessing APAP-induced hepatotoxicity and its remediation by using hepatoprotective medicines in living cells and mice. These results enable the probe to be a promising candidate for disclosing the roles of $ONOO^-$ in the liver during drug-induced hepatotoxicity and its remediation.

Conflicts of interest

There are no conflicts to declare.

Notes and references

1 (a) A. Srivastava, J. L. Maggs, D. J. Antoine, D. P. Williams, D. A. Smith and B. K. Park, *Handb. Exp. Pharmacol.*, 2010, **196**, 165–194; (b) M. Holt and C. Ju, *Handb. Exp. Pharmacol.*, 2010, **196**, 3–27.
2 (a) L. Yuan and N. Kaplowitz, *Clin. Liver Dis.*, 2013, **17**, 507–518; (b) W. Bernal and J. Wendon, *N. Engl. J. Med.*, 2013, **369**, 2525–2534.
3 Y. Zhou, L. Yang, Z. Liao, X. He, Y. Zhou and H. Guo, *Eur. J. Gastroenterol. Hepatol.*, 2013, **25**, 825–829.
4 (a) P. Pacher, J. S. Beckman and L. Liaudet, *Physiol. Rev.*, 2007, **87**, 315–424; (b) G. Ferrer-Sueta and R. Radi, *ACS Chem. Biol.*, 2009, **4**, 161–177.
5 (a) P. B. Watkins, *Therapy*, 2010, **7**, 367–375; (b) C. Cover, A. Mansouri, T. R. Knight, M. L. Bajt, J. J. Lemasters, D. Pessayre and H. Jaeschke, *J. Pharmacol. Exp. Ther.*, 2005, **315**, 879–887.
6 (a) S. Xu, H.-W. Liu, X. Yin, L. Yuan, S.-Y. Huan and X.-B. Zhang, *Chem. Sci.*, 2019, **10**, 320–325; (b) D. Cheng, J. Peng, Y. Lv, D. Su, D. Liu, M. L. Yuan and X. Zhang, *J. Am. Chem. Soc.*, 2019, **141**, 6352–6361; (c) C.-X. Yin, K.-M. Xiong, F.-J. Huo, J. C. Salamanca and R. M. Strongin, *Angew. Chem., Int. Ed.*, 2017, **56**, 13188–13198; (d) A. Shao, Y. Xie, S. Zhu, Z. Guo, S. Zhu, J. Guo, P. Shi, T. D. James, H. Tian and W.-H. Zhu, *Angew. Chem., Int. Ed.*, 2015, **54**, 7275–7280; (e) X. Han, X. Song, F. Yu and L. Chen, *Adv. Funct. Mater.*, 2017, **27**, 1700769; (f) W. Feng, S. Feng and G. Feng, *Anal. Chem.*, 2019, **91**, 8602–8606; (g) X. Li, X. Gao, W. Shi and H. Ma, *Chem. Rev.*, 2013, **114**, 590–659; (h) M. H. Lee, J. S. Kim and J. L. Sessler, *Chem. Soc. Rev.*, 2015, **44**, 4185–4191.
7 (a) H. Li, X. Li, X. Wu, W. Shi and H. Ma, *Anal. Chem.*, 2017, **89**, 5519–5525; (b) X. Li, J. Hou, C. Peng, L. Chen, W. Liu and Y. Liu, *RSC Adv.*, 2017, **7**, 34287–34292; (c) H. Zhang, J. Liu, C. Liu, P. Yu, M. Sun, X. Yan, J.-P. Guo and W. Guo, *Biomaterials*, 2017, **133**, 60–69; (d) D. Li, J. Cheng, C.-K. Wang, H. Ying, Y. Hu, F. Han and X. Li, *Chem. Commun.*, 2018, **54**, 8170–8173; (e) H. Zhang, J. Liu, Y.-Q. Sun, Y. Huo, Y. Li, W. Liu, X. Wu, N. Zhu, Y. Shi and W. Guo, *Chem. Commun.*, 2015, **51**, 2721–2724; (f) X. Jia, Q. Chen, Y. Yang, Y. Tang, R. Wang, Y. Xu, W. Zhu and X. Qian, *J. Am. Chem. Soc.*, 2016, **138**, 10778–10781; (g) Z. Li, S.-H. Yan, C. Chen, Z.-R. Geng, J.-Y. Chang, C.-X. Chen, B.-H. Huang and Z.-L. Wang, *Biosens. Bioelectron.*, 2017, **90**, 75–82; (h) J. Peng, A. Samanta, X. Zeng, S. Han, L. Wang, D. Su, D. B. Loong, N.-Y. Kang, S.-J. Park, A. All, W. Jiang, L. Yuan, X. Liu and Y.-T. Chang, *Angew. Chem., Int. Ed.*, 2017, **56**, 4165–4169.
8 (a) A. M. Pujol, M. Cuillel, O. Renaudet, C. Lebrun, P. Charbonnier, D. Cassio, C. Gateau, P. Dumy, E. Mintz and P. Delangle, *J. Am. Chem. Soc.*, 2010, **133**, 286–296; (b) H.-L. Zhang, Y. Zang, J. Xie, J. Li, G.-R. Chen, X.-P. He and H. Tian, *Sci. Rep.*, 2014, **4**, 5513; (c) Z. Li, S.-S. Deng, Y. Zang, Z. Gu, X.-P. He, G.-R. Chen, K. Chen, T. D. James, J. Li and Y.-T. Long, *Sci. Rep.*, 2013, **4**, 2293.
9 (a) Q. Duan, P. Jia, Z. Zhuang, C. Liu, X. Zhang, Z. Wang, W. Sheng, Z. Li, H. Zhu, B. Zhu and X. Zhang, *Anal. Chem.*, 2019, **91**, 2163–2168; (b) D.-T. Shi, D. Zhou, Y. Zang, J. Li, G.-R. Chen, T. D. James, X.-P. He and H. Tian, *Chem. Commun.*, 2015, **51**, 3653–3655; (c) P. Zhang, Y. Tian, H. Liu, J. Ren, H. Wang, R. Zeng, Y. Long and J. Chen, *Chem. Commun.*, 2018, **54**, 7231–7234; (d) C. Liu, Q. Duan, X. Zhang, Z. Li, P. Jia, H. Zhu, Y. Yu, Z. Wang, B. Zhu and W. Sheng, *Sens. Actuators, B*, 2019, **289**, 124–130.
10 (a) A. Bertolini, A. Ferrari, A. Ottani, S. Guerzoni, R. Tacchi and S. Leone, *CNS Drug Rev.*, 2006, **12**, 250–275; (b) B. J. Anderson, *Pediatr. Anesth.*, 2008, **18**, 915–921.
11 (a) B. L. Woolbright and H. Jaeschke, *J. Hepatol.*, 2017, **66**, 836–848; (b) M. Yan, Y. Huo, S. Yin and H. Hu, *Redox Biol.*, 2018, **17**, 274–283.
12 (a) K. de Andrade, F. Moura, J. dos Santos, O. de Araújo, J. de Farias Santos and M. Goulart, *Int. J. Mol. Sci.*, 2015, **16**, 30269–30308; (b) S. Gregory and N. D. Kelly, *Altern. Med. Rev.*, 1998, **3**, 114–127.